Journal of Alloys and Compounds 495 (2010) 268–271

Contents lists available at ScienceDirect

Journal of Alloys and Compounds

journal homepage: www.elsevier.com/locate/jallcom

A new red phosphor $LaNb_{0.70}V_{0.30}O_4:Eu^{3+}$ for white light-emitting diodes

Liya Zhou*, Junli Huang, Fuzhong Gong, Yuwei Lan, Zhangfa Tong, Jianhua Sun

School of Chemistry and Chemical Engineering, Guangxi University, Nanning, 530004, China

ARTICLE INFO

Article history:
Received 31 December 2009
Accepted 4 February 2010
Available online 11 February 2010

Keywords:
Optical materials
X-ray methods
Luminescence

ABSTRACT

A series of new red phosphors, $La_{1-x}Nb_{0.70}V_{0.30}O_4:Eu^{3+}{}_x$ ($x = 0$, 0.05, 0.10, 0.15, 0.20, 0.25, 0.30, 0.35, and 0.40), was synthesized by solid-state reaction method, and their excitation and emission spectra were measured. The $La_{0.70}Nb_{0.70}V_{0.30}O_4:Eu^{3+}{}_{0.30}$ phosphors can be efficiently excited by a ultraviolet (UV) (395 nm) source, which is coupled with the characteristic emission (350–400 nm) from UV LED (light-emitting diode). The phosphor showed intense red emission at 616 nm with good Commission internationale (CIE) chromaticity coordinates ($x = 0.660$ and $y = 0.340$), which are close to the National Television Standard Committee standard values. Meanwhile, the LED was fabricated with the $La_{0.70}Nb_{0.70}V_{0.30}O_4:Eu^{3+}{}_{0.30}$ phosphors, which can efficiently absorb ~400 nm irradiation and emit red light. Therefore, $La_{0.70}Nb_{0.70}V_{0.30}O_4:Eu^{3+}{}_{0.30}$ may find application for near UV InGaN chip-based white LEDs.

1. Introduction

Phosphor-converted light-emitting diode (LED) technique is an important solid-state illumination in which tricolor phosphors are pumped by ultraviolet (UV) InGaN chips, thereby generating white light [1–5]. With the development of LED chip technology, the emission band of LED chips has shifted from blue light (~460 nm) to near UV range (350–400 nm), with the near UV light providing higher energies to produce the phosphors [6,7]. At present, $Y_2O_2S:Eu^{3+}$ is often used as the red component for near UV InGaN-based LEDs [8]. However, this sulfide-based phosphor is chemically unstable and has low efficiency. Therefore, it is important to find a new red phosphor source that can exhibit intense red emission with high absorption in the near UV spectral region.

Recently, metal oxides that contain a transition metal without an electron in its *d* orbital, such as $NbO_4{}^{3-}$, $MoO_4{}^{2-}$, and $VO_4{}^{3-}$, have attracted much attention. This is due to their potential applications in various fields, such as phosphors, optical waveguides, and frequency doublers [9–11]. The phosphors used in the present UV LEDs were excited by about 350–400 nm photons. Eu^{3+} ions showed intense $^7F_0$–$^5L_6$ transition at 395 nm with a narrow line and could not efficiently absorb the excitation energy in some hosts because this transition is parity-forbidden. In order to strengthen and broaden the absorption around 350–400 nm, one of the important approaches is to replace the cations of the host compound. This replacement could be expected to cause a relative diversity in the sub-lattice structure around the luminescent center ions and might broaden the excitation band of the phosphor [12]. In this paper, $La_{1-x}Nb_{0.70}V_{0.30}O_4:Eu^{3+}{}_x$ red phosphors were synthesized by the solid-state reaction method, and their luminescent properties were investigated. It is known that some strong couplings between $NbO_4{}^{3-}$ and the activators Eu^{3+} exist and that efficient energy is transferred from the vanadate group $VO_4{}^{3-}$ to Eu^{3+}. Thus, the host compound can efficiently absorb the UV light and transfer the energy to the luminescent center [13,14]. The $NbO_4{}^{3-}$ and $VO_4{}^{3-}$ have equivalent value, but they have conspicuously different ionic sizes, which can result in a larger distortion on the sub-lattice structure, thus leading to the broadening and intensifying of Eu^{3+} absorption near 350–400 nm.

2. Experiment

2.1. Preparation of $La_{1-x}Nb_{1-y}V_yO_4:Eu^{3+}{}_x$ phosphors

The phosphors $La_{1-x}Nb_{1-y}V_yO_4:Eu^{3+}{}_x$ were prepared at high temperature using the solid-state reaction method. La_2O_3 (99.99%), Nb_2O_5 (99.5%), Eu_2O_3 (99.99%), and V_2O_5 (99.5%) were used as reagents for the sample preparations. All the materials were weighed at an appropriate stoichiometric ratio and grounded for at least 30 min in an agate mortar. The homogeneous mixture was then placed into a corundum crucible and sintered at 1200 °C for 5 h.

2.2. Characterization of $La_{1-x}Nb_{1-y}V_yO_4:Eu^{3+}{}_x$ phosphors

The structure of samples was examined by X-ray powder diffraction spectroscopy (XRD) under the following parameters: 40 kV, 200 mA, Cu Kα = 1.5406 Å Rigaku/Dmax – 2500. The excitation and emission spectra were recorded on a Hitachi F-2500 fluorescence spectrophotometer with a Xe lamp as the excitation source. The UV–vis spectra was measured using a UV-2501PC spectrophotometer, while the LED parameters were measured on an EVERFINE PMS-80 UV–VIS–IR spectrophotometer. All the measurements were carried out at room temperature.

---

* Corresponding author. Tel.: +86 771 3233718; fax: +86 771 3233718.
E-mail address: zhouliyatf@163.com (L. Zhou).

0925-8388/$ – see front matter © 2010 Elsevier B.V. All rights reserved.
doi:10.1016/j.jallcom.2010.02.010

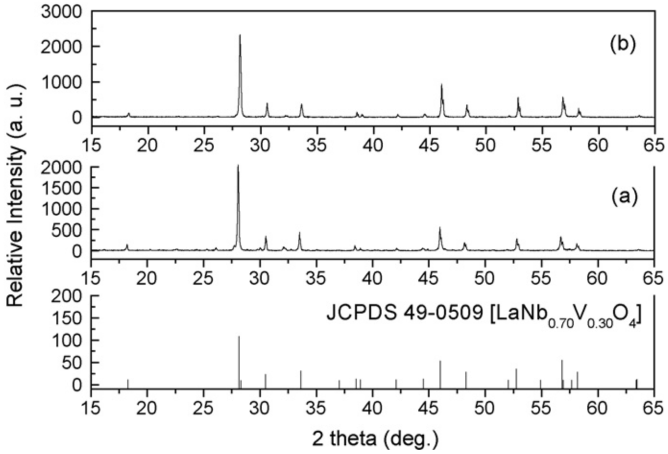

Fig. 1. XRD patterns of the $La_{0.95}Nb_{0.70}V_{0.30}O_4$:$Eu^{3+}{}_{0.05}$ phosphor sintering at (a):1100 °C, (b): 1200 °C.

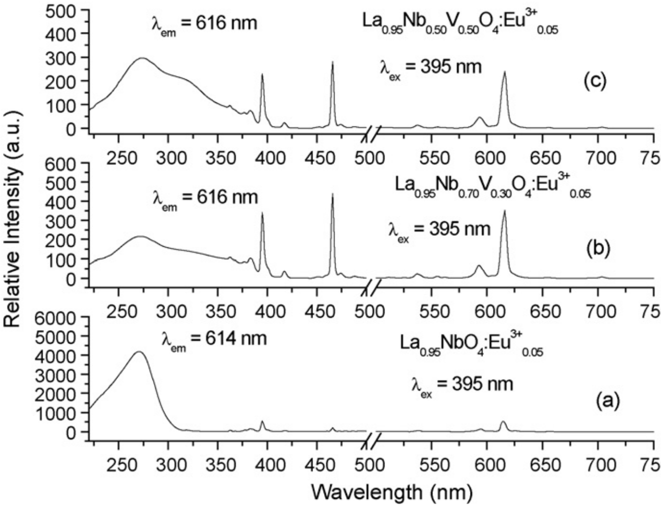

Fig. 3. Excitation and emission spectra of (a) $La_{0.95}NbO_4$:$Eu^{3+}{}_{0.05}$ (b) $La_{0.95}Nb_{0.70}V_{0.30}O_4$:$Eu^{3+}{}_{0.05}$ and (c) $La_{0.95}Nb_{0.50}V_{0.50}O_4$:$Eu^{3+}{}_{0.05}$ phosphors, respectively.

3. Results and discussion

3.1. X-ray powder diffraction characterization

The XRD patterns of $La_{0.95}Nb_{0.70}V_{0.30}O_4$:$Eu^{3+}{}_{0.05}$ samples, which were prepared using the solid-state method and sintered at different temperatures, are shown in Fig. 1a and b. The crystalline phase of the tetragonal structure appeared after it was sintered at 1100 °C. When the temperature was increased from 1100 °C to 1200 °C, the XRD patterns of the samples were observed to be consistent with those given in Joint Committee on Powder Diffraction Standards (JCPDS) 49-0509 [$LaNb_{0.70}V_{0.30}O_4$], and the intensity of the peaks became stronger because of the increased crystallinity. Due to the different valence states and ion sizes between Nb^{5+} (0.048 nm), V^{5+} (0.036 nm), and Eu^{3+} (0.107 nm), Eu^{3+} is expected to occupy the La^{3+} (0.116 nm) sites in this phosphor [11,15].

The powder XRD patterns of $La_{0.95}NbO_4$:$Eu^{3+}{}_{0.05}$ (a), $La_{0.95}Nb_{0.70}V_{0.30}O_4$:$Eu^{3+}{}_{0.05}$ (b), and $La_{0.95}Nb_{0.50}V_{0.50}O_4$:$Eu^{3+}{}_{0.05}$ (c) samples after being sintered at 1200 °C are shown in Fig. 2. Phosphors (a) and (b) are of single phase and are consistent with JCPDS 22-1125 [$LaNbO_4$] and JCPDS 49-0509 [$LaNb_{0.70}V_{0.30}O_4$], respectively. When the concentration of V^{5+} increased from 0.30 to 0.50, new diffraction peaks appeared at around 27.74° and 30.04° (2θ), indicating that the tetragonal structure of $LaNb_{0.70}V_{0.30}O_4$ is affected by the over-doping of V^{5+} ions.

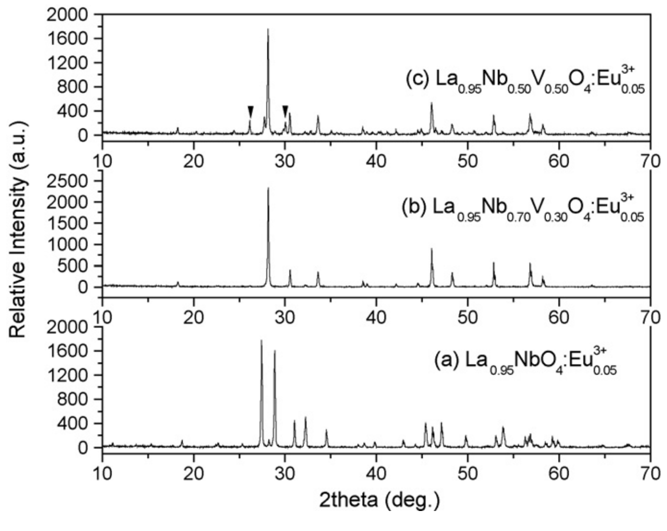

Fig. 2. The powder XRD patterns of (a) $La_{0.95}NbO_4$:$Eu^{3+}{}_{0.05}$, (b) $La_{0.95}Nb_{0.70}V_{0.30}O_4$:$Eu^{3+}{}_{0.05}$ and (c) $La_{0.95}Nb_{0.50}V_{0.50}O_4$:$Eu^{3+}{}_{0.05}$ samples, respectively.

3.2. Photoluminescent properties

The excitation and emission spectra of the $La_{0.95}NbO_4$:$Eu^{3+}{}_{0.05}$ (a), $La_{0.95}Nb_{0.70}V_{0.30}O_4$:$Eu^{3+}{}_{0.05}$ (b), and $La_{0.95}Nb_{0.50}V_{0.50}O_4$:$Eu^{3+}{}_{0.05}$ (c) samples after being sintered at 1200 °C are shown in Fig. 3. In spectra (a), there were two broad and strong excitation bands in the range of 220–320 nm. The bands centered at 223 nm and 270 nm. The peak at 270 nm was ascribed to the charge transfer (CT) state resulting from the transition of the ligand O^{2-} 2*p* orbit to the empty states of 4*f* configuration ($O^{2-} \rightarrow Eu^{3+}$). The band at around 223 nm can be attributed to the host charge transfer transition from the O^{2-} ligands to the empty 4*d* orbitals of the Nb (V) ions [13]. The transition of Eu^{3+} 4*f* configuration appearing in the long wavelength UV region of the 320–500 nm range had no effective absorption, indicating that the effective energy absorption mainly took place in the narrow UV region of 220–320 nm. In the excitation spectrum of phosphor $La_{0.95}Nb_{0.70}V_{0.30}O_4$:$Eu^{3+}{}_{0.05}$, there was a broad excitation band from 220 nm to 350 nm with a maximum at about 270 nm (Fig. 3b). This band was clearly ascribed to the CT bands of $O^{2-} \rightarrow Eu^{3+}$ and $O^{2-} \rightarrow Nb^{5+}$. The charge transferred from the O^{2-} ligands to the V^{5+} inside the $VO_4{}^{3-}$ ion was also near 260 nm, which corresponds to the transitions from the $^1A_2$ ground state to the $^1A_1$ and ^1E excited states [14]. However, the CT band of $O^{2-} \rightarrow V^{5+}$ was not clearly observed, which can be attributed to the possible overlap with the CT bands of $O^{2-} \rightarrow Eu^{3+}$ and $O^{2-} \rightarrow Nb^{5+}$. The sharp lines in the 360–500 nm range were intra-configurational 4*f*–4*f* transitions of Eu^{3+} in the host lattices, and the strong excitation bands at ∼395 nm and ∼466 nm were attributed to the $^7F_0 \rightarrow {}^5L_6$ and $^7F_0 \rightarrow {}^5D_2$ transitions of Eu^{3+}, respectively. For the $La_{0.95}Nb_{0.70}V_{0.30}O_4$:$Eu^{3+}{}_{0.05}$ phosphor, the excitation band broadened to longer wavelengths (350–400 nm) with the doping of V^{5+}. These wavelength shifts occurred due to the extra absorption of the CT bands and the efficient energy transfer from $VO_4{}^{3-}$ to Eu^{3+}, which made the intensity of the excitation band relatively strong in the near UV (NUV) region and the phosphors suitable for LED applications. When the concentration of V^{5+} increased from 0.30 to 0.50, the widths of the excitation band at around 400 nm did not increase significantly and the intensity of 395 nm decreased. From the XRD data,

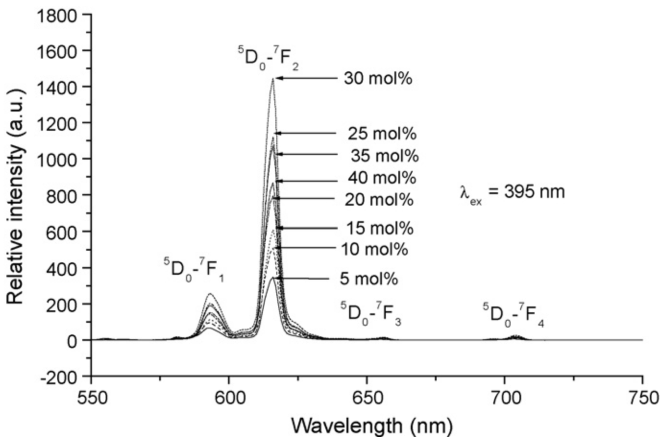

Fig. 4. Emission spectra of $LaNb_{0.70}V_{0.30}O_4$:Eu^{3+} phosphors with different Eu^{3+} doping ratios.

$LaNb_{0.50}V_{0.50}O_4$ phosphor does not contain a single phase, thus $LaNb_{0.70}V_{0.30}O_4$ was chosen as the host.

Upon excitation with 395 nm NUV irradiation, the emission spectra consisted of the well-known $^5D_0 \rightarrow {}^7F_J$ (J = 0, 1, 2, etc.) lines of Eu^{3+}. The most intense emission line was located at 614 nm or 616 nm, which corresponds to the forced electric transition of Eu^{3+} $^5D_0 \rightarrow {}^7F_2$, indicating the absence of inversion symmetry of the sites occupied by Eu^{3+} ions [16]. A ratio between the integrated intensity of these two transitions, I_{0-2}/I_{0-1}, was used in lanthanide-based systems as a probe of the local cation surroundings [17]. As shown in Fig. 3, the transition $^5D_0 \rightarrow {}^7F_2$ was much stronger than the transition $^5D_0 \rightarrow {}^7F_1$, and the ratios of I_{0-2}/I_{0-1} were about 5.60 ($La_{0.95}Nb_{0.70}V_{0.30}O_4$:$Eu^{3+}_{0.05}$) and 4.17 ($La_{0.95}NbO_4$:$Eu^{3+}_{0.05}$), respectively. This suggests that the Eu^{3+} is located in a distorted (or asymmetric) cationic environment. Other transitions from the $^5D_0 \rightarrow {}^7F_1$, $^5D_0 \rightarrow {}^7F_3$, and $^5D_0 \rightarrow {}^7F_4$, located at the range of 570–750 nm, were relatively weak, which is advantageous for obtaining saturated Commission internationale (CIE) chromaticity. The CIE chromaticity coordinates of the phosphors were calculated to be x = 0.648 and y = 0.351 ($La_{0.95}Nb_{0.70}V_{0.30}O_4$:$Eu^{3+}_{0.05}$); x = 0.649 and y = 0.351 ($La_{0.95}Nb_{0.50}V_{0.50}O_4$:$Eu^{3+}_{0.05}$); and x = 0.643 and y = 0.356 ($La_{0.95}NbO_4$:$Eu^{3+}_{0.05}$), which were close to the National Television Standard Committee (NTSC) standard values (x = 0.670 and y = 0.330).

The dependence of the Eu^{3+} doping concentration (x) in the $La_{1-x}Nb_{0.70}V_{0.30}O_4$:$Eu^{3+}_x$ (x = 0, 0.05, 0.10, 0.15, 0.20, 0.25, 0.30, 0.35, and 0.40) phosphors on the relative PL intensity at the highest $^5D_0 \rightarrow {}^7F_2$ transition is shown in Fig. 4. All of the samples $La_{1-x}Nb_{0.70}V_{0.30}O_4$:$Eu^{3+}_x$ have similar PL spectra, except for their relative intensity. This indicates that the doping concentration of Eu^{3+} ions did not alter the host structure. It can be observed that the PL emission intensity is enhanced with the increase of the Eu^{3+} doping ratio and reaches a maximum value at x = 0.30. In contrast, when the Eu^{3+} doping ratio is higher than 30 mol%, the luminescence intensity is reduced. This quenching process is often attributed to energy migration among Eu^{3+} ions. Therefore, the optimum mole concentration of Eu^{3+} in $La_{1-x}Nb_{0.70}V_{0.30}O_4$:$Eu^{3+}_x$ phosphors in this work is 30 mol%.

3.3. Characterization of UV–vis absorption spectrum

The UV–vis absorption spectrum of the $La_{0.70}Nb_{0.70}V_{0.30}O_4$:$Eu_{030}{}^{3+}$ phosphor was shown in Fig. 5. The absorption band at around 320 nm originated from oxygen to the conduction band, which was mainly composed of the d orbital of the transition metals and the CT band of $O^{2-} \rightarrow Eu^{3+}$ [9]. The absorption peaks at 395 nm and 466 nm are due to the f–f electron transitions of Eu^{3+} ions, which was consistent with the conclusion of the excitation spectrum analysis.

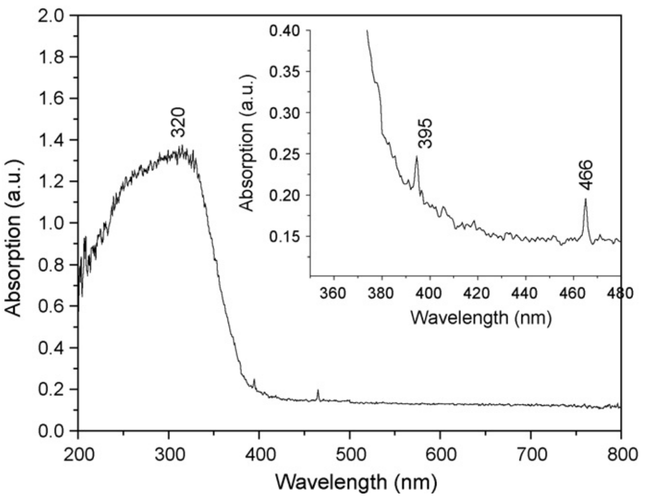

Fig. 5. UV–vis absorption spectrum of $La_{0.70}Nb_{0.70}V_{0.30}O_4$:$Eu^{3+}_{0.30}$ phosphor. Inset: detail of the absorption peaks at 395 nm and 466 nm.

3.4. Fabrication of LED with the $La_{0.70}Nb_{0.70}V_{0.30}O_4$:$Eu^{3+}_{0.30}$ phosphor

A LED was fabricated by coating the $La_{0.70}Nb_{0.70}V_{0.30}O_4$:$Eu^{3+}_{0.30}$ phosphor onto a 395 nm-emitting InGaN chip. The emission spectra of the original 395 nm-emitting InGaN chip (a) and the red-emitting LED with $La_{0.70}Nb_{0.70}V_{0.30}O_4$:$Eu^{3+}_{0.30}$ (b) under 20 mA forward bias are shown in Fig. 6. The band ~395 nm was attributed to the emission of the InGaN chip, and the sharp peaks at 594 nm, 615 nm, 655 nm, and 704 nm were originated by the absorption of the coated phosphor of $La_{0.70}Nb_{0.70}V_{0.30}O_4$:$Eu^{3+}_{0.30}$. Bright red light from the LED was observed by the naked eyes. Its CIE chromaticity coordinates were x = 0.6366 and y = 0.3247. Since the $La_{0.70}Nb_{0.70}V_{0.30}O_4$:$Eu^{3+}_{0.30}$ can efficiently absorb the ~400 nm excitation energy that the InGaN chip emitted and since its CIE chromaticity coordinates are close to the NTSC standard values, it is considered to be a good candidate for the red component of LED application.

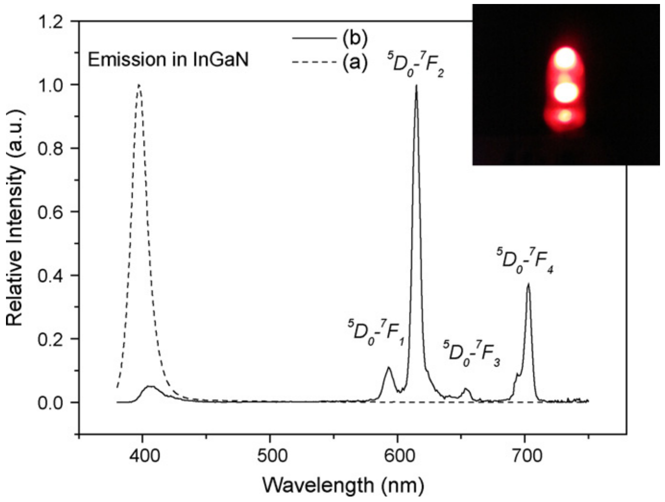

Fig. 6. Emission spectra of the original 395 nm-emitting InGaN chip (a) and the red-emitting LEDs with $La_{0.70}Nb_{0.70}V_{0.30}O_4$:$Eu^{3+}_{0.30}$ (b) under 20 mA forward bias. Inset: the photograph of the white LED-based $La_{0.70}Nb_{0.70}V_{0.30}O_4$:$Eu^{3+}_{0.30}$.

4. Conclusions

Eu^{3+}-doped $LaNb_{0.70}V_{0.30}O_4$ phosphors were prepared using the solid-state reaction. The obtained $La_{0.70}Nb_{0.70}V_{0.30}O_4$:$Eu^{3+}{}_{0.30}$ phosphors had a stronger excitation band at around 350–400 nm and enhanced red emissions due to Eu^{3+} *f–f* transitions under 395 nm light excitation. The CIE chromaticity coordinates ($x = 0.660$ and $y = 0.340$) of the phosphor were close to the NTSC standard values. The excitation band broadened to longer wavelengths with the doping of V^{5+}. There was efficient energy transfer from $VO_4{}^{3-}$ to Eu^{3+}, which made the intensity of the excitation band relatively strong at 350–400 nm. This red phosphor is suitable to be used for NUV InGaN-based LEDs. The fabricated LED further proved that the $La_{0.70}Nb_{0.70}V_{0.30}O_4$:$Eu^{3+}{}_{0.30}$ phosphors can efficiently absorb ~400 nm irradiation and emit red light that can be observed by the naked eyes. It is thus considered to be a good candidate for LED application.

Acknowledgements

This work was financially supported by grants from the Science Foundation of Guangxi (No. 0731014), Innovation Project of Guangxi Graduate Education (105930903025); the large-scale instrument of Guangxi cooperates and shares the network (496-2007-075).

Appendix A. Supplementary data

Supplementary data associated with this article can be found, in the online version, at doi:10.1016/j.jallcom.2010.02.010.

References

[1] N. Narendran, Y. Gu, J.P. Freyssinier-Nova, Y. Zhu, Phys. Status Solidi A 202 (2005) R60–R62.

[2] Z.C. Wu, L. Jie, M.L. Gong, Chem. Phys. Lett. 466 (2008) 88–90.

[3] S. Chawla, N. Kumar, H. Chander, J. Lumin. 129 (2009) 114–118.

[4] P. Li, Z. Wang, Z. Yang, Q. Guo, X. Li, Mater. Lett. 63 (2009) 751–753.

[5] D. Jia, X. Wang, Opt. Mater. 30 (2007) 375–379.

[6] J. Llanos, R. Castillo, W. Alvarez, Mater. Lett. 62 (2008) 3597–3599.

[7] Z.C. Wu, J.X. Shi, J. Wang, M.L. Gong, Q. Su, Solid State Chem. 179 (2006) 2356–2360.

[8] S. Neeraj, N. Kijima, A.K. Cheetham, Chem. Phys. Lett. 387 (2004) 2–6.

[9] T.H. Fang, Y.J. Hsiao, Y.S. Chang, Y.H. Chang, Mater. Chem. Phys. 100 (2006) 418–422.

[10] T.K. Park, H.C. Ahn, S.I. Mho, J. Korean Phys. Soc. 52 (2008) 431–434.

[11] Y.H. Wang, Y.K. Sun, J.C. Zhang, Z.P. Ci, Z.Y. Zhang, L. Wang, Physica B 403 (2008) 2071–2075.

[12] Z.L. Wang, H.B. Liang, J. Wang, M.L. Gong, Q. Su, Mater. Res. Bull. 43 (2008) 907–911.

[13] X.Z. Xiao, B. Yan, J. Non-Cryst. Solids 351 (2005) 3634–3639.

[14] X.Q. Su, B. Yan, J. Alloys Compd. 421 (2006) 238–273.

[15] D. Lide, The CRC Handbook of Chemistry and Physics on CD-ROM, CRC Press, Version 2002, 2002, pp. 12–13.

[16] S. Shionoya, W.M. Yen, Phosphor Handbook, CRC Press, Boca Raton, 1999, pp. 190–191.

[17] J.P. Rainho, L.D. Carlos, J. Rocha, J. Lumin. 87–89 (2000) 1083–1086.